

# UC Irvine

## UC Irvine Electronic Theses and Dissertations

### Title

Manipulation of Single Particles in a Solid-State Pore: Deformation of Hydrogel Particles, Diffusion, and Repeated Translocations

### Permalink

<https://escholarship.org/uc/item/7q32n93d>

### Author

Schiel, Matthew

### Publication Date

2014

### Copyright Information

This work is made available under the terms of a Creative Commons Attribution-NonCommercial-ShareAlike License, available at <https://creativecommons.org/licenses/by-nc-sa/4.0/>

Peer reviewed|Thesis/dissertation

UNIVERSITY OF CALIFORNIA,  
IRVINE

Manipulation of Single Particles in a Solid-State Pore:  
Deformation of Hydrogel Particles, Diffusion, and Repeated Translocations

THESIS

submitted in partial satisfaction of the requirements  
for the degree of

MASTER OF SCIENCE

in Biomedical Engineering

by

Matthew Schiel

Thesis Committee:  
Professor Zuzanna S. Siwy, Chair  
Professor Kenneth J. Shea  
Professor Peter J. Burke

2014

© 2014 Matthew Schiel

## TABLE OF CONTENTS

	Page
LIST OF FIGURES	iii
ACKNOWLEDGMENTS	iv
ABSTRACT OF THE THESIS	v
INTRODUCTION	1
METHODS	2
CHAPTER 1: Particle Deformation during Hydrogel Particle Translocation	4
CHAPTER 2: Diffusion of Single Particles	9
CHAPTER 3: Repeated Translocation of a Single Particle	17
CONCLUSIONS	21
REFERENCES	22

## LIST OF FIGURES

		Page
Figure 1	Gold Replicas of PET Pores	3
Figure 2	Rigid Sphere and Hydrogel Particle Translocations	6
Figure 3	Hydrogel Particle Diameter in Different Diameter Pores	7
Figure 4	Hydrogel Particle Event Durations, Peak Times, and Decay Times	8
Figure 5	Process of Balancing Voltage and Hydrostatic Pressure	10
Figure 6	Measuring Diffusion and Electrophoresis of Single Particles	14
Figure 7	Mean Square Displacement of Particles during Diffusion	15
Figure 8	Multiple Single Particle Translocations with a Set Trigger Level	18
Figure 9	Voltage Waveform used for Many Single Particle Translocations	19
Figure 10	Many Single Particle Translocations with a Signal Change Threshold	20

## **ACKNOWLEDGMENTS**

I would like to express the deepest appreciation to my committee chair, Professor Zuzanna Siwy. Without her guidance this thesis would not have been possible. I would also like to thank my committee members, Professor Kenneth Shea and Professor Peter Burke. I would like to thank Matthew Pervanik for teaching me how to do particle recordings, and everyone else in our lab for their support as well.

I also thank the American Chemical Society for permission to include copyrighted photographs as part of my thesis.

## **ABSTRACT OF THE THESIS**

Manipulation of Single Particles Moving through a Solid-State Pore:  
Deformation of Hydrogel Particles, Diffusion, and Repeated Translocations

By

Matthew Schiel

Master of Science in Biomedical Engineering

University of California, Irvine, 2014

Professor Zuzanna S. Siwy, Chair

The use of membranes with a single pore to measure particles as they pass through is a promising method to allow the rapid determination of properties of individual particles in solution. However, this will involve an understanding and control of the forces that these particles undergo while in the pore. In this work we use single cylindrical pores in PET membranes to test and compare the translocations of deformable hydrogel particles and rigid polystyrene spheres. We find that the hydrogel particles cause a characteristic initial increase in current, pass by electroosmosis, and can also undergo dehydration and deformation in pores of smaller diameter. We also show that the force on a particle by an applied hydrostatic pressure gradient can be sufficiently balanced with a transmembrane voltage that is dynamically triggered when the particle enters the pore, and the subsequent fluctuations in the current from the particle diffusing within the pore can be observed for tens of seconds. Finally, we show that repeated translocations of a single particle can be performed using a set rising edge or falling edge triggered voltage wave, or an even greater number of repetitions can be achieved by subtracting in real time the capacitance effects based on a previous test pulse.

## INTRODUCTION

In recent years there has been rapid progress in applying single pores to the study of particles and molecules. The basic setup consists of a membrane with a single pore that is used to separate two electrolyte reservoirs. An electrode is placed in each reservoir and connected to an amplifier, so that a voltage can be applied across the pore and a very small ionic current through the pore can be measured. When a particle enters the pore, it can block some of the current, leading to a resistive pulse.<sup>1</sup> One of the promises of new technologies based on using pores such as these is the ability to rapidly and with little or no prior processing investigate particle solutions at the level of single particles. This entails characterizing different types of particles as well as understanding the effects of forces on them inside the pore. Additionally, manipulating these forces while the particle is in the pore may offer new ways of testing particles. Along these lines, we sought to determine how the translocations of deformable hydrogel particles through a pore differed from those of rigid polystyrene spheres.<sup>2</sup> Secondly, we examined the process of diffusion that particles undergo in these pores, when other forces are sufficiently balanced.<sup>3</sup> Finally, we sought to expand the capabilities of testing individual particles by repeatedly passing a single particle through the pore, in alternating forward and reverse directions.



## METHODS

We fabricated single pores in Polyethylene Terephthalate (PET). First, 12  $\mu\text{m}$  thick films of polyethylene terephthalate (PET) were irradiated by single energetic heavy ions (e.g., 11.4 MeV/u Au and U ions) at the UNILAC linear accelerator of the GSI Helmholtzzentrum für Schwerionenforschung, Darmstadt, Germany, followed by chemical etching.<sup>4,5</sup> A chemical etching in 0.5 M NaOH, 70 °C was used to open the pores. Under these etching conditions, the pores will have an undulating pore diameter along the pore axis and will be symmetric (the pore opening diameter at both ends will be similar). This can be seen when gold is electrodeposited in a multi-pore membrane and the membrane is removed, as in Figure 1.<sup>1</sup> The average pore diameter was next estimated from the current–voltage measurements performed in 1 M KCl using the relationship between the pore diameter and conductance. This etching process during pore preparation also leads to a thinning of the membrane. Thus in our calculations we consider the pore length to be 11  $\mu\text{m}$ . Walls of PET pores are known to have a negative surface charge due to the presence of carboxyl groups.<sup>6</sup>

We also used several types of particles in these experiments. 410 nm in diameter carboxylated and 400 nm uncharged polystyrene particles were used (Bangs Laboratories, Fisher, IN). In addition, hydrogel particles were synthesized by a procedure adapted from Debord and Lyon<sup>7,8</sup> and described by Pervarnik et al<sup>2</sup>. NIPAm (83 mol %), AAc (5 mol %), TBAm (10 mol %), BIS (2 mol %), and SDS (10 mg) were dissolved in water (50 mL), and then were filtered through a no. 2 Whatman filter paper. TBAm (10 mol %) was dissolved in ethanol (1 mL) and then added to the monomer solution, which had a total concentration

of 65 mM. Nitrogen gas was bubbled through the reaction mixtures for 30 min. After APS aqueous solution was added (30 mg in 500  $\mu\text{L}$  of water), the prepolymerization mixture was sealed with nitrogen gas. Polymerization was carried out leaving the flask containing the prepolymerization mixture in an oil bath preset to 60 C for 3 h and then it was purified by dialysis against an excess amount of pure water for 4 days. Ion Current Recordings with the pores were made using the amplifier Axopatch 200B and 1322A Digidata (Molecular Devices, Inc.). To apply our voltage waveforms custom-written Matlab code was designed to control an Agilent 33250A Arbitrary Waveform Generator, which was then connected to one of the command voltage inputs of the Axopatch 200B. For triggering, a high-pass filtered signal was used along with a threshold trigger in the Clampex 9.2 software (Molecular Devices, Inc.).

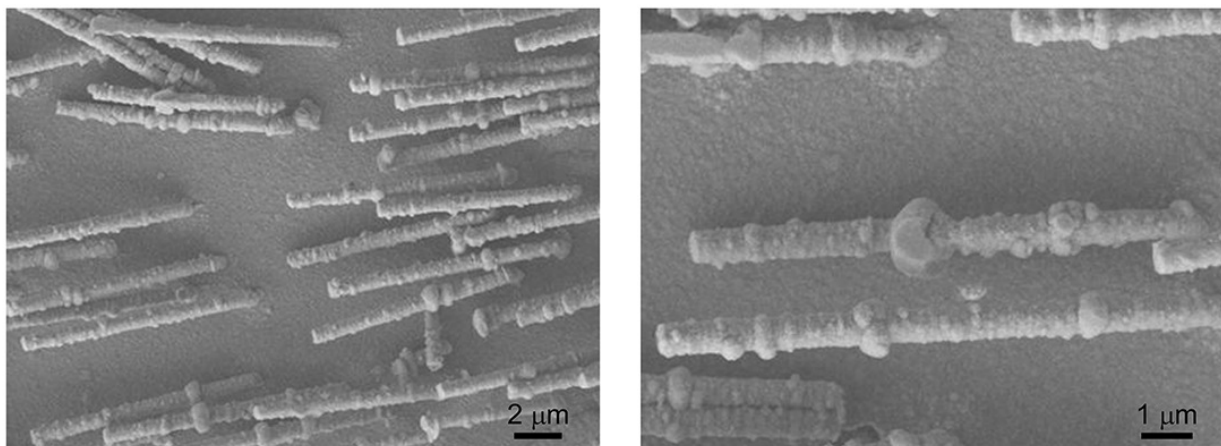


**Figure 1:** SEM images of gold replicas of similar PET pores. Gold was electrodeposited into the pores, and then the PET membrane dissolved so that the interior of the pores could be imaged. This process necessitated using membranes containing 107 pores/cm<sup>2</sup> to acquire suitable images in a reasonable time. These membranes were etched under the same conditions as the single-pore membranes used for particle translocations. Reprinted with permission from Pervarnik et al (2012)<sup>1</sup>. Copyright 2012 American Chemical Society.

## Chapter 1

### Particle Deformation during Hydrogel Particle Translocation

First, translocations of two types of particle were compared, 220 nm diameter carboxylated polystyrene spheres and ~300 nm diameter hydrogel particles, through a 12 micron long track-etched PET pore of diameter 540 nm. The particle sizes were initially measured under different ionic concentrations with a Zetasizer Nano ZS (Malvern Instruments, Westborough, MA). The polystyrene spheres were found to be 220 nm and showed no dependence on salt concentrations. The hydrogels were found to be 320 nm, 300nm, and 260 nm in 1 mM, 10mM, and 0.1 M KCl, respectively. These KCl solutions were all buffered to pH 10 with 10mM Tris and were also 0.01% Tween 80 by volume. At this pH the hydrogel particles become negatively charged and swell due to the deprotonation of carboxyl groups within the hydrogel network.<sup>8</sup>

The polystyrene particles are a model for hard spheres, and do not deform as they pass through the pore. As expected, they caused a resistive pulse by blocking some of the ionic current. The undulating pore diameter is also reflected in the shape of this pulse (Figure 2c). This basic shape was preserved for all of these particle events at different voltages and concentrations, supporting the idea that it indeed reflects the pore topography.<sup>1</sup> The polystyrene particles translocated primarily due to electrophoresis, where their negative charge caused them to move toward the positive electrode.

Though the hydrogel particles were also negatively charged, they had a lower zeta potential (-24 +/- 8.0 mV) than the polystyrene particles (-47 +/- 9.0 mV), and translocated under the reverse bias primarily by electroosmosis toward the negative electrode. In fact,

while the pulse still showed a similar pore shape, they created a current increase instead of a decrease (Figure 2d and e). This is most likely due to the low density structure of the hydrogel with its negative charge, which can bring a large number of cations along with it into the pore. In effect the conductance within the hydrogel is higher than the bulk solution, so the resistance of the pore system is reduced when the particle enters. However, during the course of the translocation, near the end of the event, the current then gradually decreased to a level below the baseline current. A similar pattern was seen in experiments with deformable microgels passing through glass pipettes under pressure-driven flow, where the current decrease was only observed with pipettes of diameter smaller than the particles. This was explained as a combination of dehydration and deformation of the particles.<sup>2,9,10</sup>

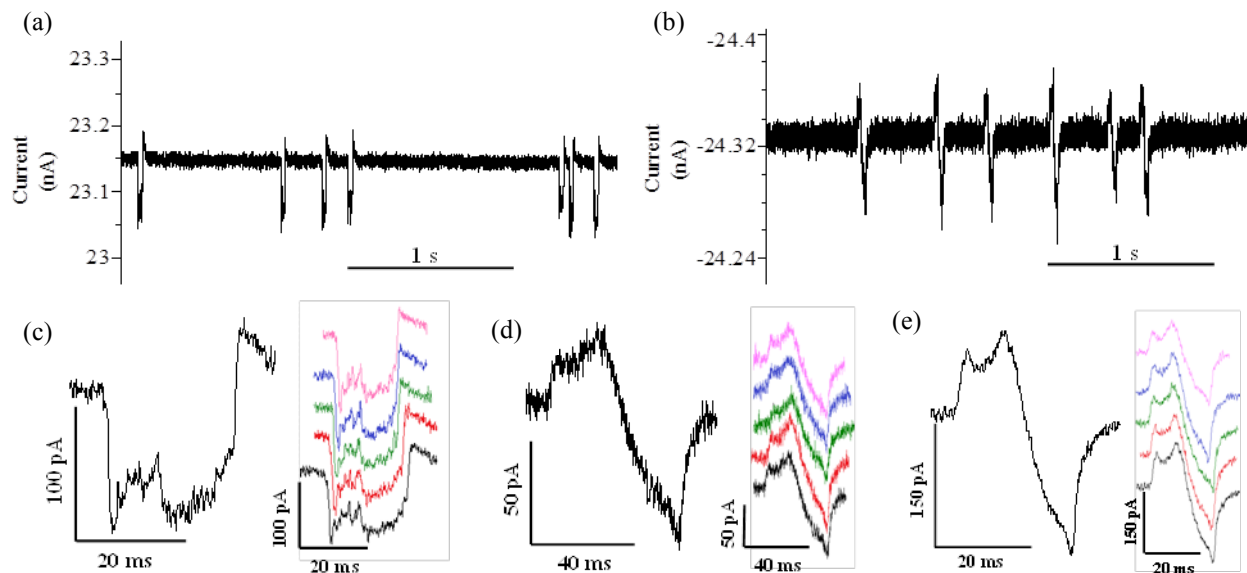


**Figure 2:** Ionic current versus time for a 540 nm diameter pore at (a) +1000 mV and (b) -1000 mV in 100 mM KCl, 10 mM Tris (pH 10), and 0.01% Tween 80: (a) 220 nm diameter hard spheres (polystyrene particles modified with carboxyl groups) translocate electrophoretically through the pore; (b) ~300 nm diameter hydrogels pass through the pore by electroosmosis. Magnified view of these ionic current pulses for (c) the rigid spheres at +1000 mV, (d) the hydrogel particles at -1000 mV, and (e) the hydrogel particles at -2000 mV. A single event is shown on the left, while the right shows five events, vertically offset from each other to facilitate comparison. Reprinted with permission from Pervarnik et al (2013)<sup>2</sup>. Copyright 2013 American Chemical Society.

To further investigate the factors at work during the passage of the hydrogel particles, we then tested them using pores of different average diameters, from 1600 nm down to 200 nm. The particles were only seen to pass through pores larger than 330 nm, and they always passed by electroosmosis, not electrophoresis. The events all had a current increase followed by a decrease below the baseline, as seen earlier. To quantify the effects of dehydration and deformation, the effective particle size was calculated using the amplitude of the current decreases with the known average pore diameter, and is shown in Figure 3. At pore diameters below 500 nm there is a large reduction in the effective particle size, to below 280 nm, suggestion that in this regime the hydrogel particles underwent dehydration and deformation.<sup>2</sup>

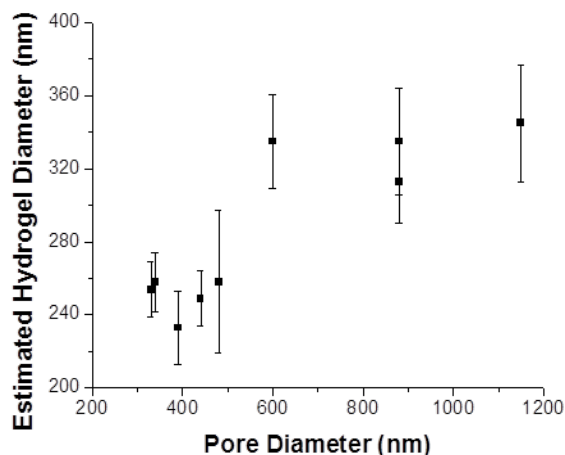


**Figure 3:** Size of the hydrogels as a function of the pore diameter. The hydrogel diameter was estimated from the depth of the resistive pulses in 10 mM KCl, pH 10, and 0.01% Tween 80 and calculated as described in ref 7. The hydrogel hydrodynamic diameter as measured by dynamic light scattering was 300 nm at 20 °C (10 mM KCl, pH 10). Reprinted with permission from Pervarnik et al (2013)<sup>2</sup>. Copyright 2013 American Chemical Society.

We also analyzed the effect of pore diameter on the pulse duration, which is related to the particle velocity as it translocates through the pore. For the hard spheres, the pulse duration was seen to increase as the pore diameter decrease. This is due to a larger drag force on the particle as the distance between it and the pore wall is reduced.

For the hydrogel particles, the relationship between the pulse duration and pore diameter was more complicated. We characterized this in terms of three different times within each event: (i) the time to peak, which was the time from the start of the event until the peak decrease in current, (ii) the peak decay time, which was the time from the peak decrease until it returned to the baseline current (within 10% of the change in current at the peak), and (iii) the total event duration, which was the sum of times (i) and (ii) (see Figure 4). We observed that at large pore diameters, all three times increased with decreasing diameters, but below 500 nm this trend reversed, and then below 350 nm the

trend reversed again. Below 350 nm the decay time also actually became longer than the time to peak.<sup>2</sup> In the future planned studies, the three times will be correlated with the degree of cross-linking of the particles, which regulates the particle stiffness. If such correlation could be established, the resistive-pulse technique with rough pores could also be used for studying mechanical properties on an individual particle basis.

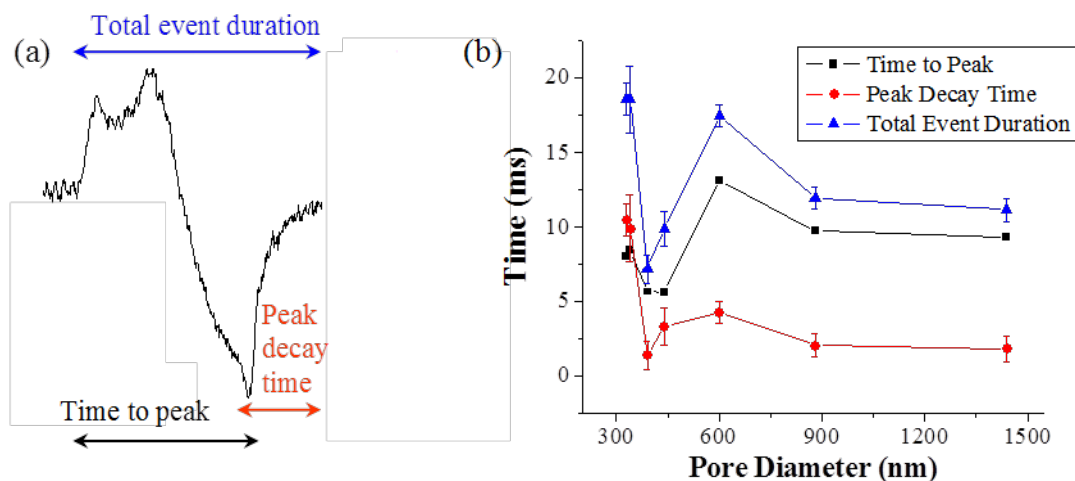


**Figure 4:** (a) Three times used to characterize duration of resistive pulses obtained with hydrogels translocating through pores of different diameters. The black symbols represent the time needed to reach the lowest value of the current, the red symbols indicate the time needed to reach the baseline current from the lowest value, and the blue symbols are the sum of the two. (b) Resistive pulse durations as shown in (a) for pores of different diameters recorded at  $-2$  V. All experiments were performed in 10 mM KCl, pH 10, and 300 nm diameter hydrogels. Reprinted with permission from Pervarnik et al (2013)<sup>2</sup>. Copyright 2013 American Chemical Society.

## Chapter 2

### Diffusion of Single Particles

To begin studying the diffusion of single particles, we used 410 nm carboxylated polystyrene spheres and a pore with an average diameter of 720nm. The particles and the pore walls are both negatively charged, so they travel with a combination of electrophoresis and electroosmosis. However, their movement was always toward the positive electrode, and thus their transport was dominated by electrophoresis. To allow the translocation to occur at small voltages, below 1V, we used a high ionic strength of 0.2 M KCl.<sup>11</sup> These low electric fields also lengthened the translocation times to tens of milliseconds.

To observe diffusion, we realized the ion current fluctuations could be monitored when the forces applied to the particle were sufficiently balanced. Then as the particle moved left or right along the pore axis due to diffusion, it would pass by different diameter openings of the pore, leading to changes in the ion current. However, if no transmembrane was applied at all, then any of these current changes would be less than the noise of the system. We therefore needed to keep a non-zero voltage applied, to ensure the signal could be measured. We decided to use hydrostatic pressure, by placing different electrolyte levels on either side of the membrane, in order to balance this required voltage. Also by starting with a pressure gradient, the voltage could be easily fine-tuned to achieve this balance, as illustrated in Figure 5. We set the level of the electrolyte with the particles 3mm higher than the level of only KCl on the other side, and particles were driven through the pore using a voltage of -40mV. We then used an ion current decrease, the resistive pulse from a single particle entering the pore, to trigger a square wave voltage applied from



a function generator with a set delay, to allow the particle to move farther into the pore, and a constant amplitude of 100mV. The DC offset of this voltage wave was then manually shifted from a starting value of zero by steps of  $\sim 1$  mV after each particle event until the hydrostatic pressure was counterbalanced, at 60mV in the example shown in Figure 5. Once this offset was adjusted like this, the majority of the particles did not leave the pore even after 40 seconds (obvious fluctuations in the ion current continued). In fact the particles were driven out of the pore when the voltage of -40mV was reapplied. Using the Einstein-Smoluchowski equation, the bulk diffusion coefficient of 410 nm particles can be calculated as  $D_{\text{bulk}}=1.1 \times 10^{-12} \text{ m}^2/\text{s}$ . Assuming one-dimensional diffusion, according to the

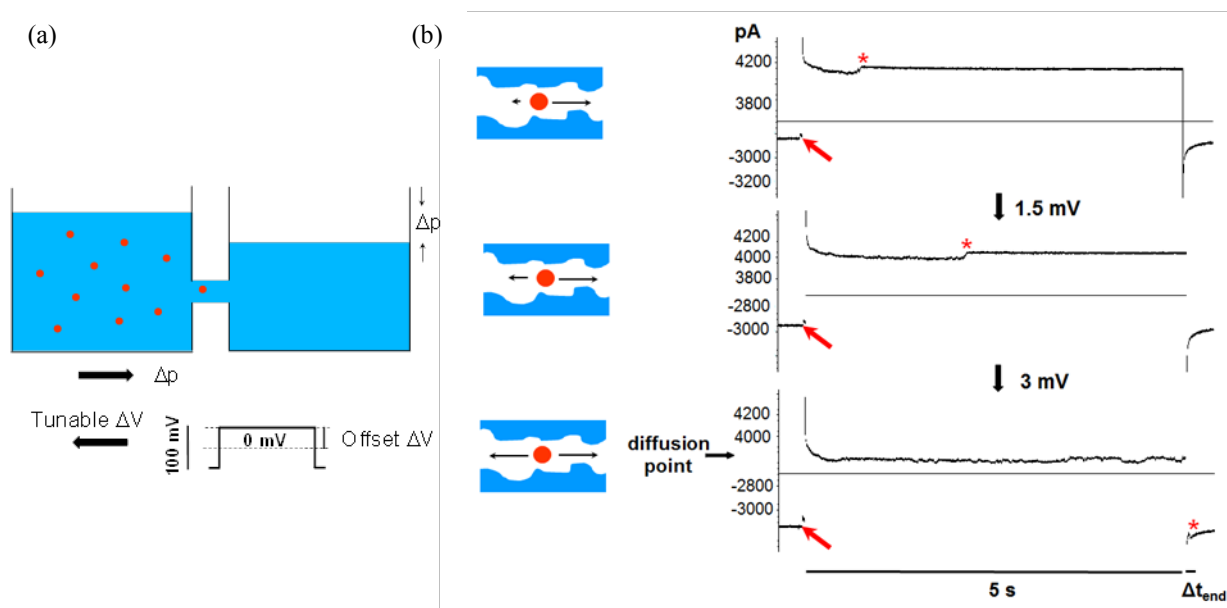


**Figure 5:** Process of adjusting voltage across the membrane to counterbalance the hydrostatic pressure difference,  $\Delta p$ . (a) Electrolyte level in the chamber of the conductivity cell containing the particles was 0.3 cm higher compared to the electrolyte level in the other chamber filled with KCl. (b) Applied square voltage wave with tunable offset  $\Delta V$  and duration is applied to counterbalance  $\Delta p$ . The recordings were performed in 0.2 M KCl, pH 10, using 410 nm particles passing through 720 nm in diameter pore. Red arrows mark the beginning of the current pulse thus particle entrance to the pore; the red star indicates the particle exit. When changing  $\Delta V$  with  $\sim 1$  mV steps, conditions were found when  $\Delta V$  (60 mV) balanced  $\Delta p$  (the bottom panel), and the particle exited the pore only when the driving voltage ( $-40$  mV) was reapplied. For higher values of  $\Delta V$ , the particle exited the pore within a few seconds. The insets indicate the directions of the particle motion. When the forces are balanced, the particles can move in both directions. Reprinted with permission from Schiel et al (2014)<sup>3</sup>. Copyright 2014 American Chemical Society.

first passage time relation of  $L^2/2D_{\text{bulk}}$ , the particle would take ~60 seconds to diffuse through the entire length of the pore,  $L=11\mu\text{m}$ .<sup>12</sup> Since in our experiments, the diffusion of the particle is allowed to start when it is some distance inside the pore, it starts at a smaller distance than  $L$  from either side. However, the known reduction in the diffusion coefficient compared to the bulk solution when confined within a pore<sup>13-18</sup> explains why the particles were still diffusing even after 40 seconds in the pore.<sup>3</sup>

As evidence that the forces were balanced, we estimated the velocity that would be induced by the hydrostatic pressure, as well as the velocity from the applied voltage. The 3mm difference in the fluid levels corresponds to a  $\Delta P \sim 30\text{Pa}$ . Then the average pressure induced velocity can be calculated from the Poiseuille relation:

$$v_{\text{pressure}} = \frac{\Delta P R^2}{8\eta L}$$

where  $R$  is the pore radius,  $L$  is the pore length ( $11\mu\text{m}$ ), and  $\eta$  is the solution viscosity. The calculated  $v_{\text{pressure}}$  for  $\Delta P = 30\text{Pa}$ , and  $R = 360\text{nm}$ , is  $45\mu\text{m/s}$ .<sup>19</sup>

When voltage is applied across a pore with charged pore walls, the particles' transport occurs by a combination of electroosmosis and electrophoresis. In case of a thin electrical double-layer, the net electrokinetic velocity can be found as

$$v_{\text{electrokinetic}} = \left(\frac{\varepsilon}{\eta}\right)(\zeta_{\text{particle}} - \zeta_{\text{pore}})E$$

where  $\zeta_{\text{particle}}$  and  $\zeta_{\text{pore}}$  are zeta potentials of the particle and pore walls, respectively,  $\epsilon = \epsilon_0 \epsilon_r$ , and  $E$  stands for electric field calculated as the applied voltage divided by the pore length.<sup>20</sup> The zeta potential of 410 nm was measured to be  $\zeta_{\text{particle}} -25 \text{ mV}$ ,<sup>1</sup> and based on reported measurements of zeta potential of porous polymer membranes<sup>21-23</sup> and known reduction of  $\zeta$  by Tween 80,<sup>1</sup> the value of  $\zeta_{\text{pore}}$  was estimated to be  $-10 \text{ mV}$ . With these zeta potentials values and an applied voltage of  $60 \text{ mV}$ , the  $v_{\text{electrokinetic}}$  is found to be  $40 \mu\text{m/s}$ , which is very close to the  $v_{\text{pressure}}$  of  $45 \mu\text{m/s}$ . These velocities,  $v_{\text{electrokinetic}}$  and  $v_{\text{pressure}}$ , are in opposite directions, thus validating that the forces on the particle in the pore were sufficiently balanced.<sup>3</sup>

We then used the procedure in Figure 5 in experiments which allowed the particles to diffuse for a certain length of time, from 10 ms and 10 s, in order to find the diffusion coefficient of the particles using mean square displacement.<sup>12</sup> We set the time for each particle to diffuse using the length of the square wave. The displacement during diffusion could be determined for each particle by comparing the electrokinetic displacements before and after the diffusion pause with the total pore length (see Figure 6). Thus we determined the time that the particle travelled into the pore before the voltage was switched,  $\Delta t_{\text{start}}$  (which was set to  $\sim 1/5$  of the total translocation time before starting our experiments), and the time it took the particle to leave the pore after the voltage was switched back,  $\Delta t_{\text{end}}$ . Both these durations were found after removing the capacitance discharge from the recorded trace that had been created by each switch in the voltage.<sup>3,24</sup>

To find the electrokinetic velocity of each particle in the pore, we assumed the velocity was independent of position and measured the time,  $\Delta t_{\text{total}}$ , the particle would need to translocate if the voltage remained on for the complete translocation ( $-75 \text{ mV}$ , the

baseline voltage, Figure 6). After the full diffusion pause and the particle was driven out of the pore, the same particle was driven back to the starting point under a reversed voltage and then driven once again at  $-75$  mV (Figure 6a), giving us the pulse of duration  $\Delta t_{\text{total}}$ . The displacement during diffusion of the particle in the pore could then be calculated as the electrokinetic velocity times the difference between  $\Delta t_{\text{total}}$  and  $(\Delta t_{\text{start}} + \Delta t_{\text{end}})$ . The electrokinetic velocity at  $-75$  mV of  $150 \mu\text{m/s}$  was 800 times higher than the speed during diffusion, which was calculated from the bulk diffusion coefficient (a distance of  $11 \mu\text{m}$  in the bulk is diffused over 60 second), confirming that the electrokinetics was dominate at  $-75\text{mV}$ . Since variation in the time  $\Delta t_{\text{total}}$  and therefore the electrokinetic velocity was very small among different particles ( $\Delta t_{\text{total}} = 74 \pm 4$  ms at  $-75$  mV), all our subsequent experiments were performed without measuring the electrokinetic translocation for each individual particle. This sped up the analysis, thus allowing us to look at a larger population of particles and as well as a larger set of diffusion times required to obtain viable measurements of diffusion coefficients. Using a library of 200 electrokinetic events collected beforehand, a full electrokinetic translocation was matched to the electrokinetic portions of each event containing a diffusion recording.<sup>3</sup>

The mean square displacement (MSD) as a function of time is shown in Figure 7 for  $410$  nm particles diffusing in a another pore, which had a diameter of  $1100$  nm. The undulations in the pore diameter were of similar magnitude to the previous  $720$  nm pore we had been using, so the variations of particle velocity along the pore axis were not expected to exceed 20%. A least 40 different, individually diffusing particles were used to calculate each value of the MSD, after the mean displacement had been removed. Figure 7 was created with a total of 348 particles of  $410$  nm (black squares). The diffusion

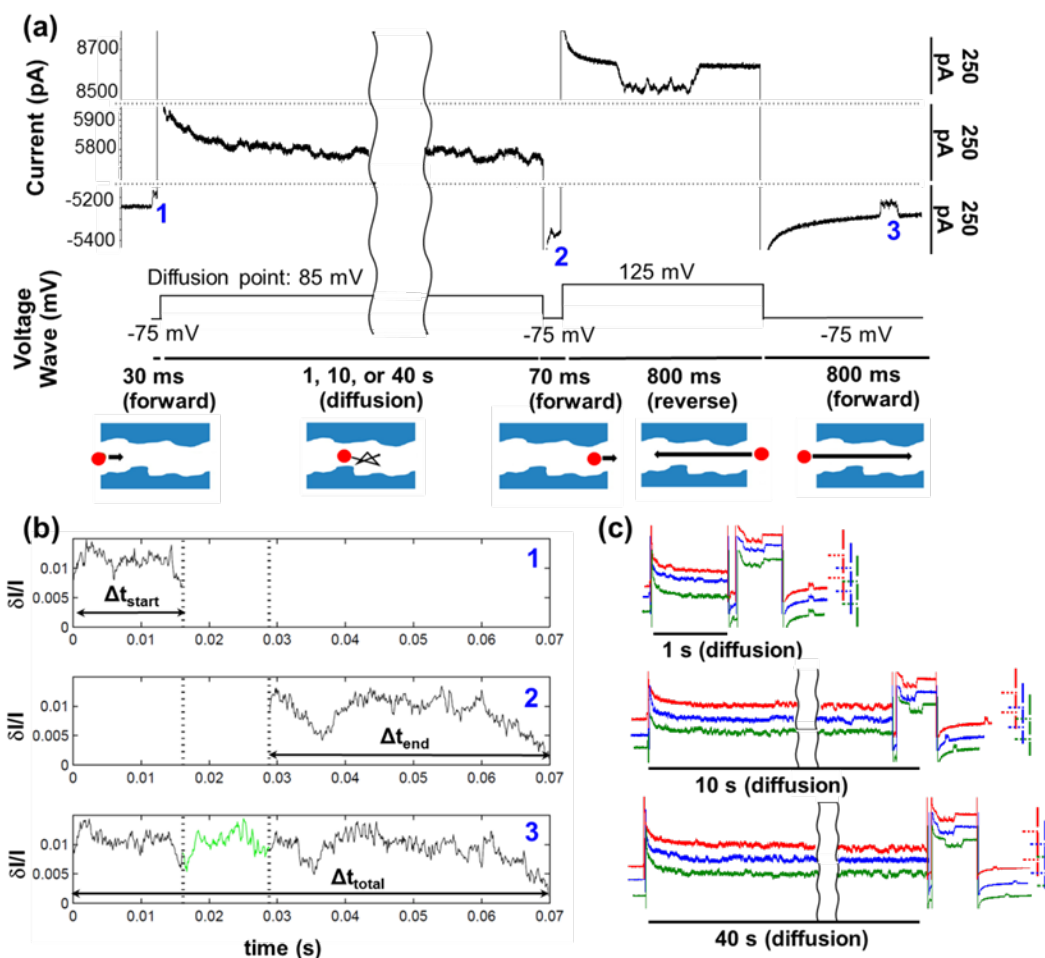


**Figure 6:** Comparison of diffusive and electrophoretic transport of single 410 nm particles in a 720 nm in diameter pore. (a) The experiment was performed in a configuration shown in Figure 5 with the difference in electrolyte levels in the conductivity cell chambers of 0.5 cm, using the following sequence of applied voltages. With a set time delay,  $\Delta t_{start}$ , after the particle entered the pore, the voltage waveform was applied setting the voltage across the membrane to a value that balanced the hydrostatic pressure difference (85 mV in this experiment). The particle was allowed to diffuse for a controlled period of time up to 40 s. The original voltage was subsequently turned on for 70 ms, and the particle exited the pore. The voltage was set to a small reverse value (125 mV) for 800 ms driving the same particle back through the pore in the opposite direction. The same particle was again driven to the right using  $-75$  mV. Due to changes of the voltage value and polarity, the recorded range of ion current is wide thus to facilitate visual analysis of the recordings, there are three nonconsecutive ion current scales, separated by horizontal lines. (b) In order to estimate the diffusion displacement of each particle in the pore, three durations of time were monitored: (1)  $\Delta t_{start}$ , (2)  $\Delta t_{end}$  – time needed to complete the translocation after the particle underwent diffusion in the pore; an example of recorded data for one 10 s long diffusion pause is shown. (3)  $\Delta t_{total}$  – time needed for the particle to electrophoretically pass through the pore at the same voltage at which  $\Delta t_{start}$  and  $\Delta t_{end}$  were found. All three portions of the traces are plotted in terms of  $\delta I/I$  with the baseline due to the capacitive discharge corrected. (c) Example recordings of ion current with the diffusive pauses of 1 s, 10 s, and 40 s for the same consecutive voltage values as in (a). For each diffusive pause, recordings with three different particles are shown. All scale bars shown on the far right correspond to 250 pA with colors matching the three distinct recordings for three particles. Note that as shown in (a) there are three different current regimes shown. Reprinted with permission from Schiel et al (2014)<sup>3</sup>. Copyright 2014 American Chemical Society.

coefficient of the particles was found to be  $(1.8 \pm 0.2) \cdot 10^{-13} \text{ m}^2/\text{s}$ , given by the slope of MSD vs time, which is  $\sim 5$  lower than the value of the bulk diffusion coefficient. The offset in the graph is from the localization error (the limited precision in determination of the particle position).<sup>3,25</sup>

To further confirm the forces on the charged particles were sufficiently balanced, the MSD was measured in the same 1100 nm pore for uncharged 400 nm in diameter polystyrene particles. These particles passed through the pore primarily by electroosmosis. Independent of the charge, the diffusion coefficients of the 410 carboxylated and 400 nm unmodified polystyrene particles would be expected to be very similar. This is indeed confirmed in Figure 7 (green triangles), and suggests there was minimal residual electric

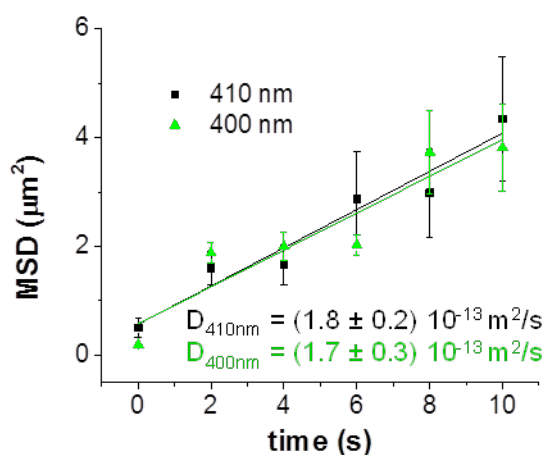


**Figure 7:** Mean square displacements of 410 nm (black squares) and 400 nm (green triangles) in diameter polystyrene particles in a 1100 nm in diameter pore as a function of diffusion time set as 10 ms, 2 s, 4 s, 6 s, 8 s, and 10 s. Black and green lines represent the linear fit to the shown points for 410 and 400 nm particles, respectively. The 410 nm in diameter particles were modified with carboxyl groups and passed through the pore in the direction of electrophoresis. The 400 nm polystyrene particles were uncharged, and their translocation occurred by electroosmosis. Reprinted with permission from Schiel et al (2014)<sup>3</sup>. Copyright 2014 American Chemical Society.

force on the particles and this did not interfere in our determination of diffusion coefficient. A total of 576 individual particles were used to determine the MSD for the 400 nm particles.<sup>3</sup>

## **Chapter 3**

### **Repeated Translocation of a Single Particle**

We next investigated the possibility of driving repeated translocations of a single particle, first with a trigger set to an absolute current level. Using a rising edge trigger with delay we were able to drive a single particle back to its starting point outside the pore, recapture it, and repeatedly apply our designed waveform on the same particle (Figure 8a). Similarly, a falling edge trigger allowed us to recapture the particle at the opposite entrance of the pore and move it back to the original position (Figure 7b) where the full event could be retriggered repeatedly and automatically. The final approach allowed us to move the particle back and forth without reaching any of the pore entrances. This involved a manual design of the voltage signal applied during the entire particle translocation in both directions (Figure 7c). The maximum and minimum value of the designed voltage wave was  $\sim 75$  mV above and  $\sim 75$  mV below the diffusive point found using the method previously shown in Figure 5.

However, using these methods the particle would normally escape after a several translocations. One primary issue was the capacitive discharge obscuring the particle signal after each voltage switch. We also wanted to combine the use of the rising and falling edge triggers. In order to facilitate more repeated translocations, we explored the possibility of subtracting the capacitance and calculating a percent signal change in the current in real time, to create a signal we could then base our trigger on. Figure 8 shows the basic setup of our voltage waveform, applied by a National Instruments PCI-6221 DAQ, and controlled with a custom written Simulink program in Matlab. There was as an initial voltage switch when the particle entered the pore, followed by a repeating pattern



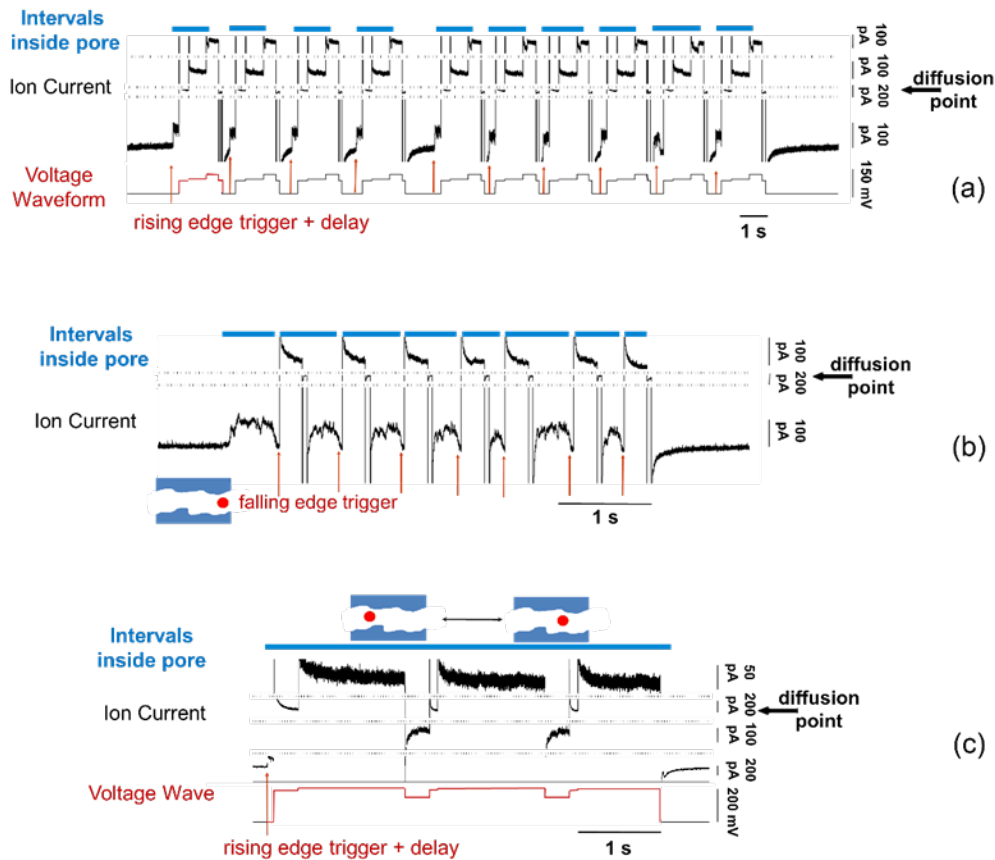


**Figure 8:** Modulation of voltage signal during particle translocation allows one to drive the same particle through a pore multiple times. Rising edge trigger with delay combined with appropriately designed voltage wave recapture the particle after the translocation is completed (a) or move the particle back and forth along the pore axis without letting it leave the pore (c). Falling edge trigger enables automatic recapture at the opposite entrance of the pore (b). The experiments were performed with 410 nm in diameter carboxylated particles and 720 nm in diameter pore. Horizontal lines in (a)–(c) indicate nonconsecutive scales of ion current. Reprinted with permission from Schiel et al (2014)<sup>3</sup>. Copyright 2014 American Chemical Society.

of 4 voltage levels (but with varying durations, since they were each triggered using the percent signal change in current). These 4 levels consisted of (i) a higher magnitude negative voltage level to recapture the particle in the forward direction, (ii) a lower magnitude negative voltage drive to the particle through the rest of the pore in the forward direction, (iii) a higher magnitude positive voltage level to recapture the particle in the reverse direction, and (iv) a lower magnitude positive voltage level to drive the particle through the rest of the pore in the reverse direction. A test pulse with a set delay for each

of these levels was first applied to pore without any triggering from the particles, to capture the capacitance discharge waveform at each level. To construct a signal to use for triggering, these capacitance signals were then set up to be subtracted in real time whenever the corresponding voltage switch occurred. The percent signal change in the current was calculated after this capacitance removal using a moving average function. Therefore, we could detect the particle leaving the pore during the lower magnitude voltage levels when the percent signal change dropped below a specified threshold and switch to the next voltage level. Likewise when signal was above a specified threshold

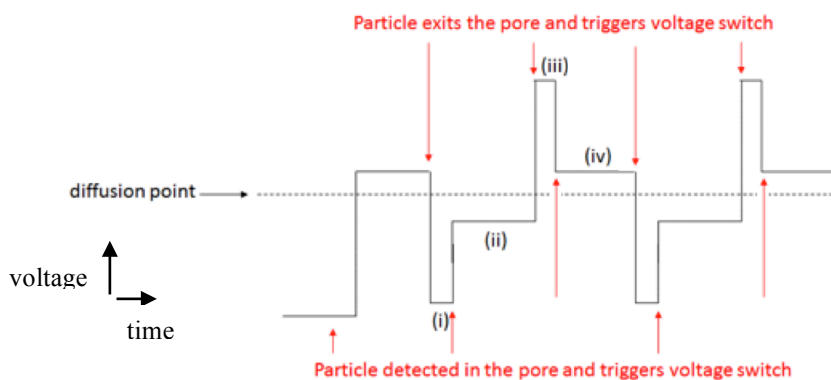


**Figure 9:** Illustration of voltage waveform applied for repeated translocations triggered by percent signal change thresholds. After the particle first enters the pore there is a delayed initial voltage switch, followed by four repeating, but varying duration, voltage levels: (i) a higher magnitude negative voltage level to recapture the particle in the forward direction, (ii) a lower magnitude negative voltage drive to the particle through the rest of the pore in the forward direction, (iii) a higher magnitude positive voltage level to recapture the particle in the reverse direction, and (iv) a lower magnitude positive voltage level to drive the particle through the rest of the pore in the reverse direction.

during the higher magnitude voltage levels this signaled that the particle had entered the pore. Additionally, we specified a minimum time for each voltage switch before the triggers became active, to avoid any residual capacitance discharge left in the signal. Using this setup we were able to record a single 410 nm particle translocating back and forth up to 80 times for 30 seconds, as shown in Figure 10.

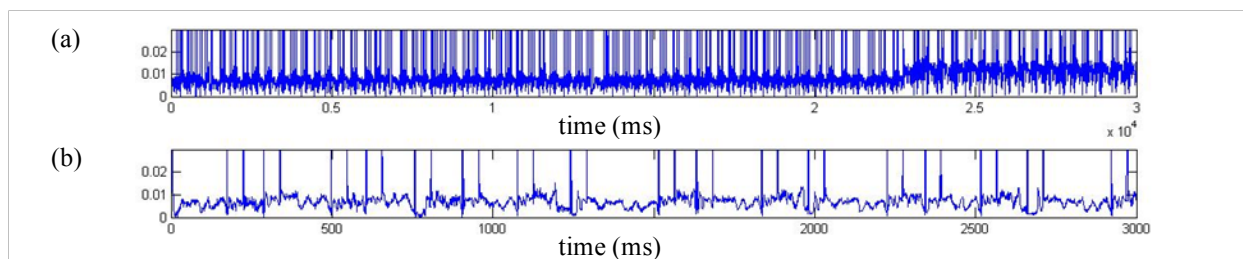


**Figure 10:** Many Translocations of a single particle using a signal change threshold. (a) A single 410nm particle is moved back and forth across the pore 80 times in 30 seconds by triggering the voltage switches with a threshold level applied to the percent signal change after the real time removal of the capacitive discharge. This percent signal change is shown. (b) A magnified view of this trace for the first 3 seconds. The large brief spikes in the percent signal change are times when the voltage was switched.

## Conclusions

In these experiments we investigated the properties of particles passing through single solid-state pores fabricated in PET membranes, and tested the ability to manipulate the forces acting on them as they passed through.

We found the hydrogel particles initially increased the conductivity through the pore, but then gradually decreased the current below the baseline. This is in contrast to the decreases seen with rigid polystyrene spheres, although the pulse shape from the undulating pore remained similar. We also found that in smaller diameter pores, these hydrogel particles show a marked reduction in their effective size, due to dehydration and deformation. Pores with longitudinal irregularities could be potentially used for quantifying mechanical properties of individual objects.

Secondly, we were able to show that the force from a pressure gradient across the pore on a particle inside the pore could be sufficiently balanced by the fine-tuning of an applied voltage across the pore. This allowed us to record the current fluctuations due to diffusion of the individual particles for up to 40 seconds. We were then also able to calculate the displacement during diffusion, by using the electrokinetic displacement when the particle entered and exited the pore compared to the full electrokinetic translocation.

Finally, we were also able to record several repeated translocations of a single particle by using voltage waveforms applied with a trigger based on an absolute threshold current level. Furthermore, we are able to achieve ten's of repeated translocations (up to 80) for periods up to 30 seconds, by using real time removal of the capacitance effects and calculation of a percent signal change in the current.

## References

1. Pevarnik, M.; Healy, K.; Toimil-Molares, M. E.; Morrison, A.; Letant, S. E.; Siwy, Z. S.; Polystyrene Particles Reveal Pore Substructure as They Translocate. *ACS Nano* **2012**, *6*, 7295-7302.
2. Pevarnik, M.; Schiel M.; Yoshimatsu, K.; Vlasiouk, I. V.; Kwon, J. S.; Shea, K. J.; Siwy, Z. S.; Particle Deformation and Concentration Polarization in Electroosmotic Transport of Hydrogels Through Pores. *ACS Nano* **2013**, *7*, 3720-8.
3. Schiel M.; Siwy, Z. S.; Diffusion and Trapping of Single Particles in Pores with Combined Pressure and Dynamic Voltage. *J. Phys. Chem. C* **2014**, *118*, 19214–19223.
4. Fleischer, R. L.; Price, P. B.; Walker, R. M. *Nuclear Tracks in Solids: Principles and Applications*; University of California Press: Berkeley, CA, 1975.
5. Spohr, R. Methods and Device to Generate a Predeter- mined Number of Ion Tracks. German Patent DE2951376 C2, Sept 15, 1983; U.S. Patent 4369370, 1983.
6. Ermakova, L. E.; Sidorova, M. P.; Bezrukova, M. E. Filtration and Electrokinetic Characteristics of Track Membranes. *Colloid J.* **1998**, *52*, 705–712.
7. Hendrickson, G. R.; Lyon, L. A. Microgel Translocation through Pores under Confinement. *Angew. Chem., Int. Ed.* **2010**, *49*, 2193–2197.
8. Debord, J. D.; Lyon, L. A. Synthesis and Characterization of pH-Responsive Copolymer Microgels with Tunable Volume Phase Transition Temperatures. *Langmuir* **2003**, *19*, 7662– 7664.
9. Holden, D. A.; Hendrickson, G. R.; Lan, W.-J.; Lyon, L. A.; White, S. H. Electrical Signature of the Deformation and Dehydration of Microgels during Translocation through Nanopores. *Soft Matter* **2011**, *7*, 8035–8040.
10. Holden, D. A.; Hendrickson, G.; Lyon, L. A.; White, H. S. Resistive Pulse Analysis of Microgel Deformation during Nanopore Translocation. *J. Phys. Chem. C* **2011**, *115*, 2999– 3004.
11. Menestrina, J.; Yang, C.; Schiel, M.; Vlasiouk, I.; Siwy, Z. S. Charged Particles Modulate Local Ionic Concentrations and Cause Formation of Positive Peaks in Resistive-Pulse-Based Detection. *J. Phys. Chem. C* **2014**, *118*, 2391–2398.
12. Berg, H. C. *Random Walks in Biology*; Princeton University Press: Princeton, NJ, 1983.
13. Bezrukov, S. M.; Vodyanoy, I.; Parsegian, V. A. Counting Polymers Moving Through a Single Ion Channel. *Nature* **1994**, *370*, 279–281.
14. Pedone, D.; Langecker, M.; Abstreiter, G.; Rant, U. A Pore – Cavity – Pore Device to Trap and Investigate Single Nanoparticles and DNA Molecules in a Femtoliter Compartment: Confined Diffusion and Narrow Escape. *Nano Lett.* **2011**, *11*, 1561–1567.
15. Larkin, J.; Henley, R. Y.; Muthukumar, M.; Rosenstein, J. K.; Wanunu, M. High-Bandwidth Protein Analysis Using Solid-State Nanopores. *Biophys. J.* **2013**, *106*, 696–704.
16. Pagliara, S.; Schwall, C.; Keyser, U. F. Optimizing Diffusive Transport Through a Synthetic Membrane Channel. *Adv. Mater.* **2013**, *25*, 844–849.

17. Eral, H. B.; Oh, J. M.; van den Ende, D.; Mugele, F.; Duits, M. H. G. Anisotropic and Hindered Diffusion of Colloidal Particles in a Closed Cylinder. *Langmuir* **2010**, *26*, 16722–16729.
18. Lin, B.; Yu, J.; Rice, S. A. Direct Measurements of Constrained Brownian Motion of an Isolated Sphere Between Two Walls. *Phys. Rev. E* **2000**, *62*, 3909–3919.
19. Landau, L. D.; Lifshitz, E. M. *Fluid Mechanics*, 2nd ed.; Reed Educational and Professional Publishing, Ltd.: New York, 1987.
20. Firnkes, M.; Pedone, D.; Knezevic, J.; Döblinger, M.; Rant, U. Electrically Facilitated Translocations of Proteins through Silicon Nitride Nanopores: Conjoint and Competitive Action of Diffusion, Electrophoresis, and Electroosmosis. *Nano Lett.* **2010**, *10*, 2162–2167.
21. Dejardin, P.; Vasina, E. N.; Berezkin, V. V.; Sobolev, V. D.; Volkov, V. I. Streaming Potential in Cylindrical Pores of Poly(ethylene terephthalate) Track-Etched Membranes: Variation of Apparent Zeta Potential with Pore Radius. *Langmuir* **2005**, *21*, 4680–4685.
22. Salgin, S.; Salgin, U.; Soyer, N. Streaming Potential Measurements of Polyethersulfone Ultrafiltration Membranes to Determine Salt Effects on Membrane Zeta Potential. *Int. J. Electrochem. Sci.* **2013**, *8*, 4073–4084.
23. Lettmann, C.; Möckel, D.; Staude, E. Permeation and Tangential Flow Streaming Potential Measurements for Elektrokinetic Characterization of Track-Etched Microfiltration Membranes. *J. Membr. Sci.* **1999**, *159*, 243–251.
24. Smeets, R. M. M.; Keyser, U. F.; Dekker, N. H.; Dekker, C. Noise in Solid-State Nanopores. *Proc. Natl. Acad. Sci. U.S.A.* **2008**, *105*, 417–421.
25. Michalet, X. Mean Square Displacement Analysis of Single- Particle Trajectories with Localization Error: Brownian Motion in an Isotropic Medium. *Phys. Rev. E* **2010**, *82*, 041914(1–13).